Article

A New HRCT Score for Diagnosing SARS-CoV-2 Pneumonia: A Single-Center Study with 1153 Suspected COVID-19 Patients in the Emergency Department

Soccorsa Sofia [1], Giacomo Filonzi [2], Leonardo Catalano [2], Roberta Mattioli [2], Laura Marinelli [1], Elena Siopis [2], Laura Colì [2], Violante Mulas [2], Davide Allegri [3], Carlotta Rotini [4], Beatrice Scala [2], Alessio Bertini [1], Michele Imbriani [2], Michele Domenico Spampinato [4,*] and Paolo Orlandi [2]

[1]   Emergency Department, Azienda Unità Sanitaria Locale di Bologna, 40137 Bologna, Italy;
      soccorsa.sofia@ausl.bologna.it (S.S.); laura.marinelli@ausl.bologna.it (L.M.);
      alessio.bertini@ausl.bologna.it (A.B.)
[2]   Radiology Department, Azienda Unità Sanitaria Locale di Bologna, 40137 Bologna, Italy;
      giacomo.filonzi@ausl.bologna.it (G.F.); leonardo.catalano@ausl.bologna.it (L.C.);
      roberta.mattioli@ausl.bologna.it (R.M.); elena.siopis@ausl.bologna.it (E.S.); laura.coli@ausl.bologna.it (L.C.);
      violante.mulas@ausl.bologna.it (V.M.); beatrice.scala@ausl.bologna.it (B.S.);
      michele.imbriani@ausl.bologna.it (M.I.); paolo.orlandi@ausl.bologna.it (P.O.)
[3]   UOC Governo Clinico e Sistema Qualità, Azienda Unità Sanitaria Locale di Bologna, 40137 Bologna, Italy;
      davide.allegri@ausl.bologna.it
[4]   Department of Translational Medicine and for Romagna, University of Ferrara, 44124 Ferrara, Italy;
      rtnclt@unife.it
*   Correspondence: spmmhl@unife.it; Tel.: +39-3803684962

Abstract: The 2019 coronavirus disease (COVID-19) pandemic is affecting millions of people worldwide. Chest high-resolution computed tomography (HRCT) is commonly used as a diagnostic test for suspected COVID-19; however, despite numerous attempts, there is no single scoring system that is widely accepted and used in clinical practice to estimate the probability of SARS-CoV-2 pneumonia. The aim of this single-center retrospective study is to develop a radiological score to predict the probability of COVID-19 with HRCT. Patients admitted to the emergency department with symptoms suggestive of COVID-19 who underwent both HRCT and RT-PCR on nasopharyngeal swab to detect SARS-CoV-2 infection between 1 March and 30 April 2020 were included. A multivariable regression analysis was conducted to identify all HRCT signs independently associated with a positive RT-PCR assay for SARS-CoV-2 and build the HRCT score. A total of 1153 patients were enrolled in this study. The number of segments with ground glass opacities (OR 1.18, 95% CI 1.11–1.26), number of segments with linear opacities (OR 1.21, 95% CI 1.05–1.42), crazy paving patterns (OR 6, 95% CI 3.79–9.76), and vascular ectasia in each segment (OR 2.46, 95% CI 1.1.5–5.8) were included in the score. The HRCT score showed high discriminatory power (area under the ROC curve of 0.8267 [95% CI 0.8–0.85]) with 72.2% sensitivity, 86.6% specificity, 78% PPV, and 83% NPV for its best cut-off. In summary, the HRCT score has good diagnostic and discriminatory accuracy for COVID-19 and is easy and quick to perform.

Keywords: SARS-CoV-2; COVID-19; scoring system; HRCT; diagnostic modality; diagnostic accuracy

1. Introduction

The pandemic COVID-19 (coronavirus disease 2019), which began with the SARS-CoV-2 (severe acute respiratory syndrome coronavirus 2) outbreak in Wuhan in December 2019, has affected millions of people worldwide. Despite the declaration of the end of the global health emergency and the lower mortality rate, millions of people are still affected by SARS-CoV-2 today, and rapid diagnosis remains of paramount importance [1]. The reference standard for COVID-19 diagnosis is the RT-PCR test, which may yield false-negative

results in some cases or require repeat testing in highly suspicious and initially negative cases [2]. Like other viruses, SARS-CoV-2 causes interstitial pneumonia, and high-resolution computed tomography (HRCT) is the best imaging modality. Various scoring systems have been proposed to assess the severity of SARS-CoV-2 pneumonia, including the chest CT severity score, the chest CT score, the total severity score, the modified total severity score, and the three-level chest severity score, showing high interobserver agreement and accuracy [3]. Ground glass opacity (GGO), crazy paving pattern, consolidations, and vascular enhancement are among the most common CT features in COVID-19, occurring predominantly in the subpleural areas and affecting mainly the lower lungs in advanced stages of the disease. This radiological pattern has been classified as typical of SARS-CoV-2 pneumonia. However, although the chest CT is recognized as a crucial tool for early diagnosis of the disease [4], few studies aimed to develop a quantitative assessment of chest imaging to predict the likelihood of SARS-CoV-2 infection. Therefore, HRCT based on qualitative assessment of the chest CT has proven to be a sensitive but moderately specific test for the diagnosis of COVID-19 that is unable to distinguish SARS-CoV-2 from other causes of pneumonia [5].

The aim of this study was to develop and validate a new HRCT score to estimate the probability of SARS-CoV-2 pneumonia in patients suspected of having COVID-19.

2. Materials and Methods

We conducted this retrospective, monocentric cohort study in the emergency department (ED) of a large, third-level hospital with >80,000 patients per year and >800 inpatient beds, designated as a national reference center for critical care in the event of a pandemic. All adult patients admitted between 1 March and 30 April 2020 with a clinical suspicion of COVID-19 and who had both a chest HRCT, lung ultrasound (LUS), and nasopharyngeal swab for RT-PCR testing for SARS-CoV-2 were included. This manuscript follows the 2015 STARD guidelines on reporting diagnostic accuracy studies [6] and the Transparent Reporting of a multivariable prediction model for Individual Prognosis Or Diagnosis (TRIPOD) statement on transparent reporting of a multivariable predictive model for an individual prognosis or diagnosis [7]. The present study was conducted in accordance with the Declaration of Helsinki and approved by the local ethics committee.

2.1. HRCT

All HRCT examinations were performed in the radiology emergency department of our hospital. Patients were examined in the supine position and during end-inspiration using a 64-section scanner CT (Ingenuity Core CT; Philips Medical Systems, Cleveland, OH, USA). The HRCT protocol included non-enhanced imaging of the chest (section thickness 2 mm). The HRCT protocol included an unenhanced image of the thorax (slice thickness, 2 mm; slice interval, 1 mm) acquired with a standard kernel and soft tissue window (400 widths; 20 centers) and a reconstruction of the parenchyma (slice thickness, 1 mm; slice interval, 0.5 mm) with a sharp kernel and lung window (1600 widths; 600 centers). The technical parameters of the CT scan were as follows: tube voltage, 120 kV; tube current modulation 120–250 mAs; spiral division factor, 0.609; matrix, 512 (mediastinal window); and 1024 (lung window). The HRCT scans of all patients participating in the study were reviewed in a blinded fashion with respect to the outcome of the RT-PCR test and the final diagnosis. Each HRCT scan was randomly reviewed by five radiologists with 15–25 years of experience and three residents with at least two years of experience. All investigators analyzed each bronchopulmonary segment for each patient and looked for the following parenchymal abnormalities according to the "Fleischner Society: Glossary of Terms for Thoracic Imaging" unless otherwise stated [8]:

-       Ground glass opacity (GGO): area of cloudy, increased lung opacity with preservation of bronchial and vascular margins (Figures 1 and 2);

-       Consolidation: homogeneous increase in lung parenchymal opacity obscuring the vascular margins and airway walls with an air bronchogram (pattern of air-filled bronchi on a background of opaque airless lung) (Figure 3);
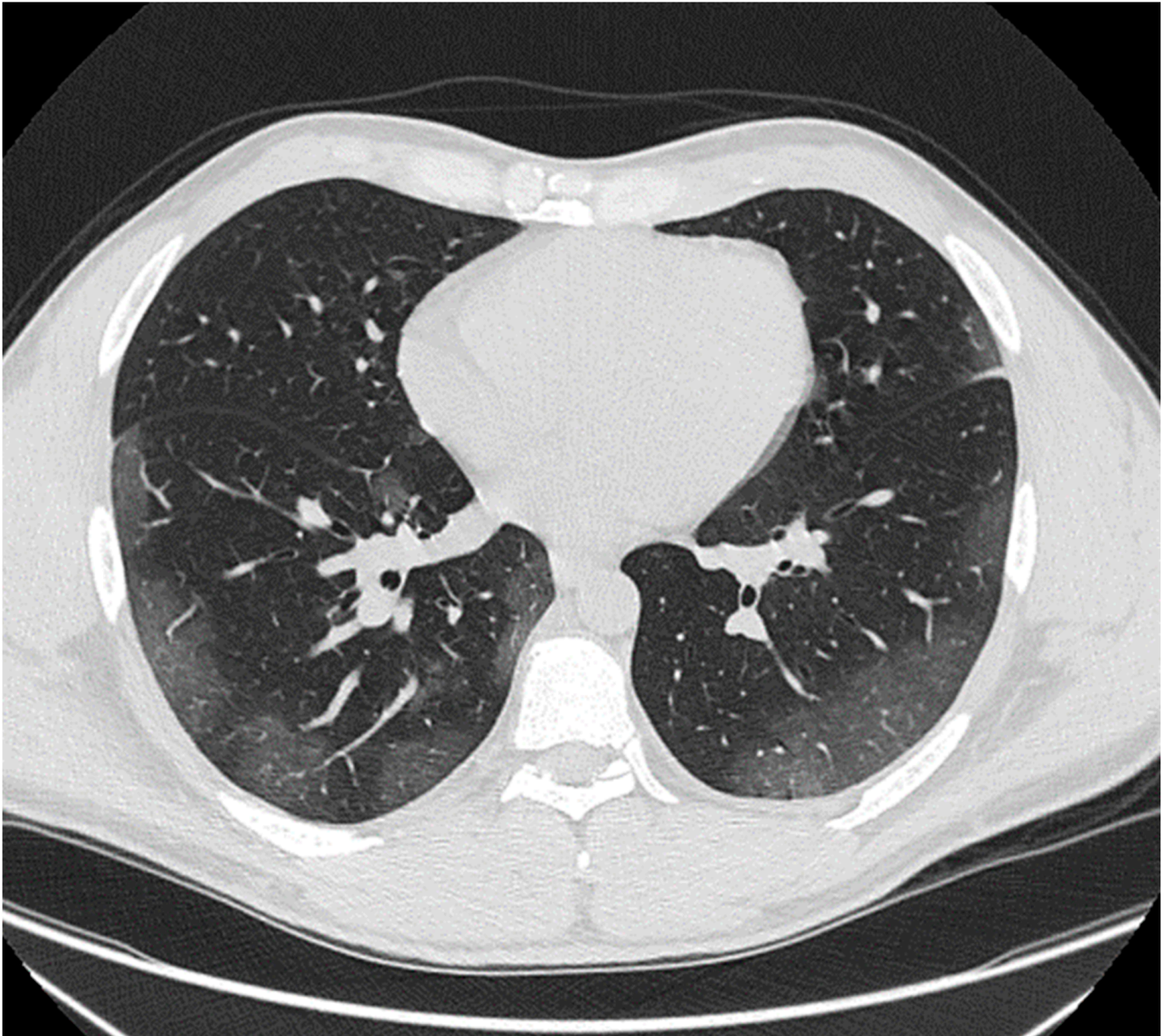

Figure 1. Axial image of HRCT of lungs in a 46-year-old male with PCR-confirmed COVID-19 pneumonia showing bilateral peripheral areas of ground glass opacities.
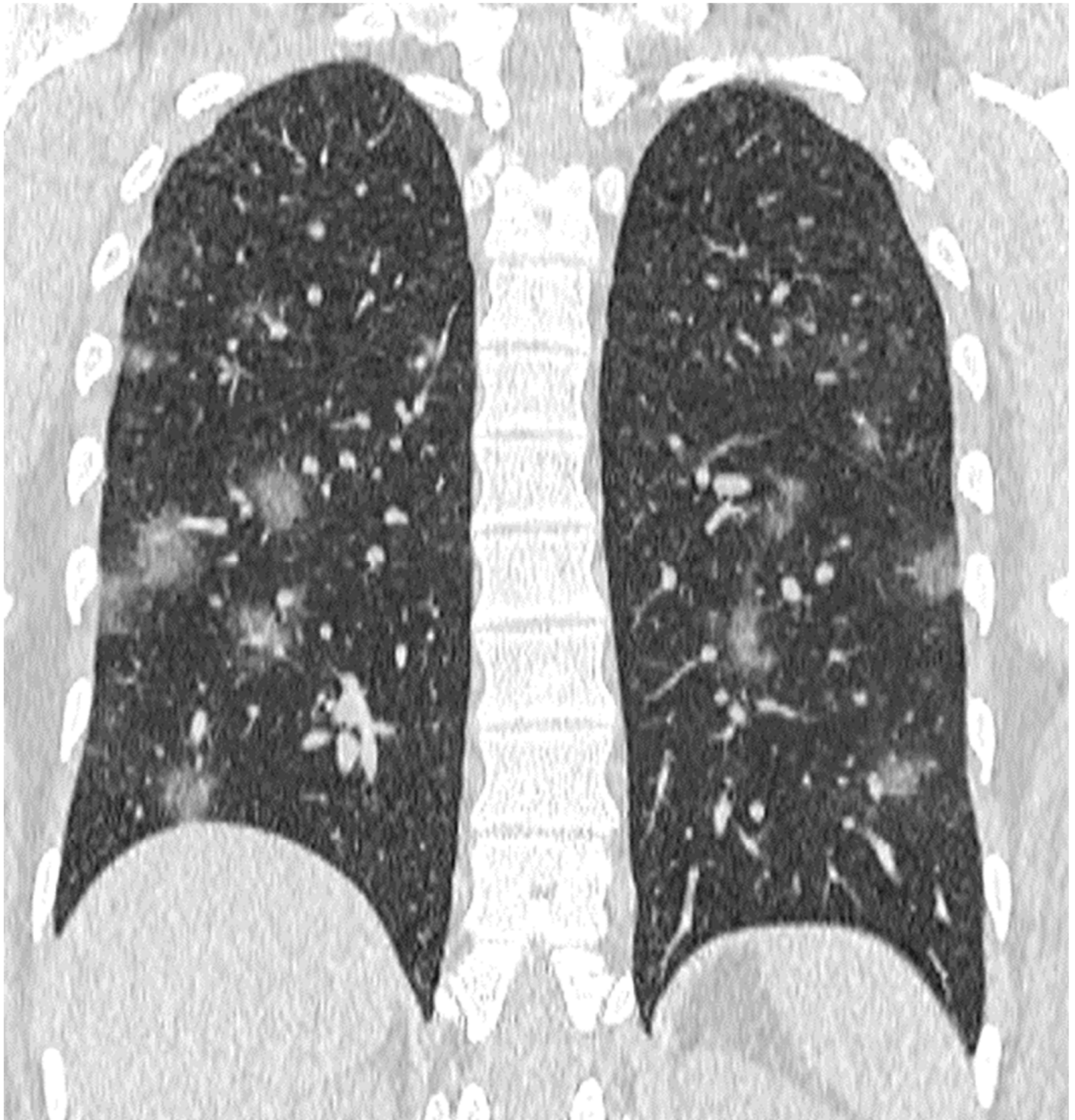
Figure 2. Coronal image of HRCT of lungs in a 29-year-old male with PCR-confirmed COVID-19 pneumonia showing bilateral small, rounded, ground glass opacities.
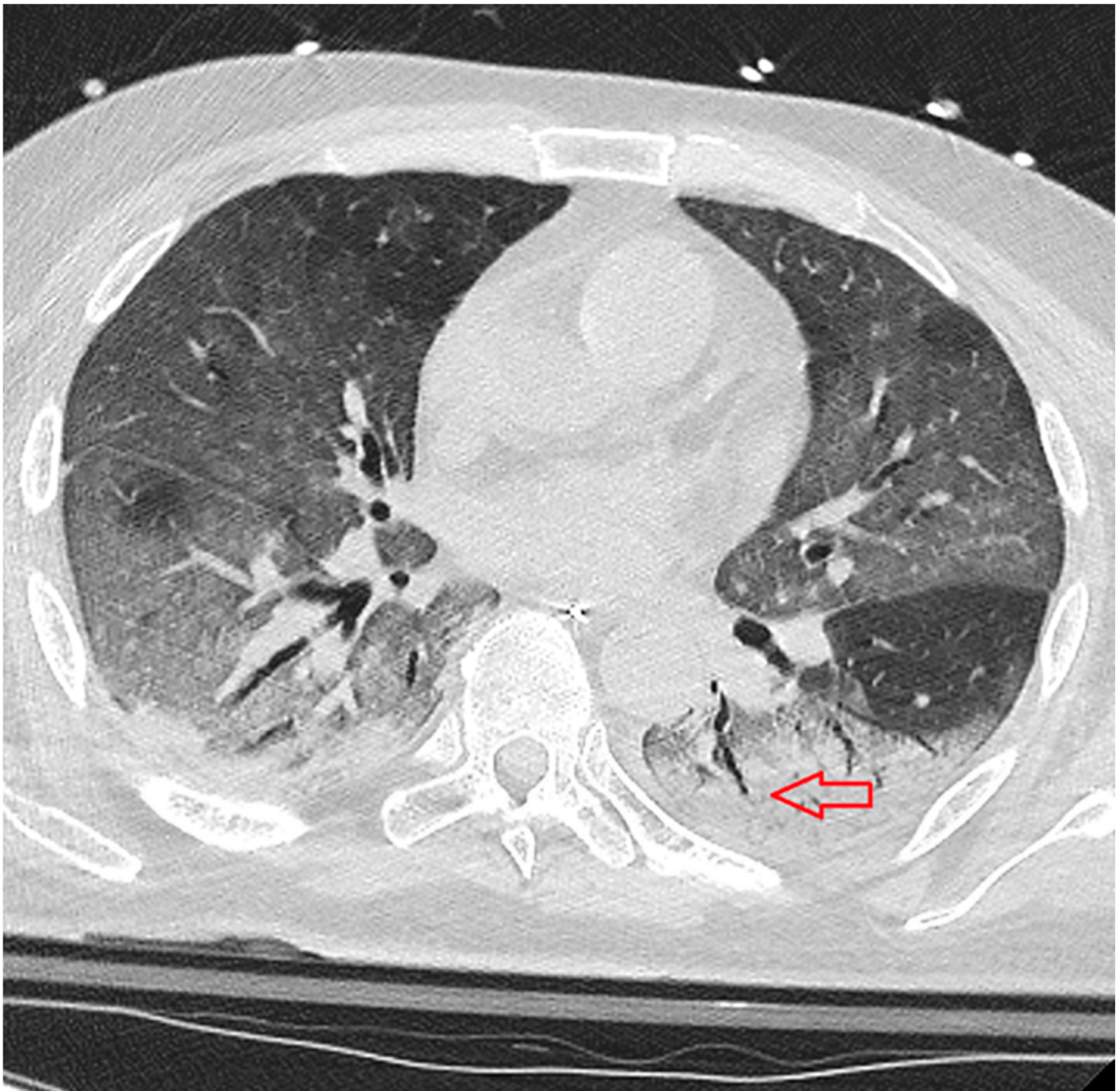
Figure 3. Axial image of HRCT of lungs in a 74-year-old woman with PCR-confirmed COVID-19 pneumonia showing bilateral areas of ground glass opacities and bilateral consolidations in dorsal areas of lower lobes, with air bronchogram (red arrow).

- Consolidation without air bronchogram;
- Subpleural curvilinear line: thin, curved opacity 1–3 mm thick, less than 1 cm from and parallel to the pleural surface (Figure 4);
- Crazy paving pattern: thickened interlobular septa and intralobular lines superimposed on a background of ground glass opacity (Figure 6);
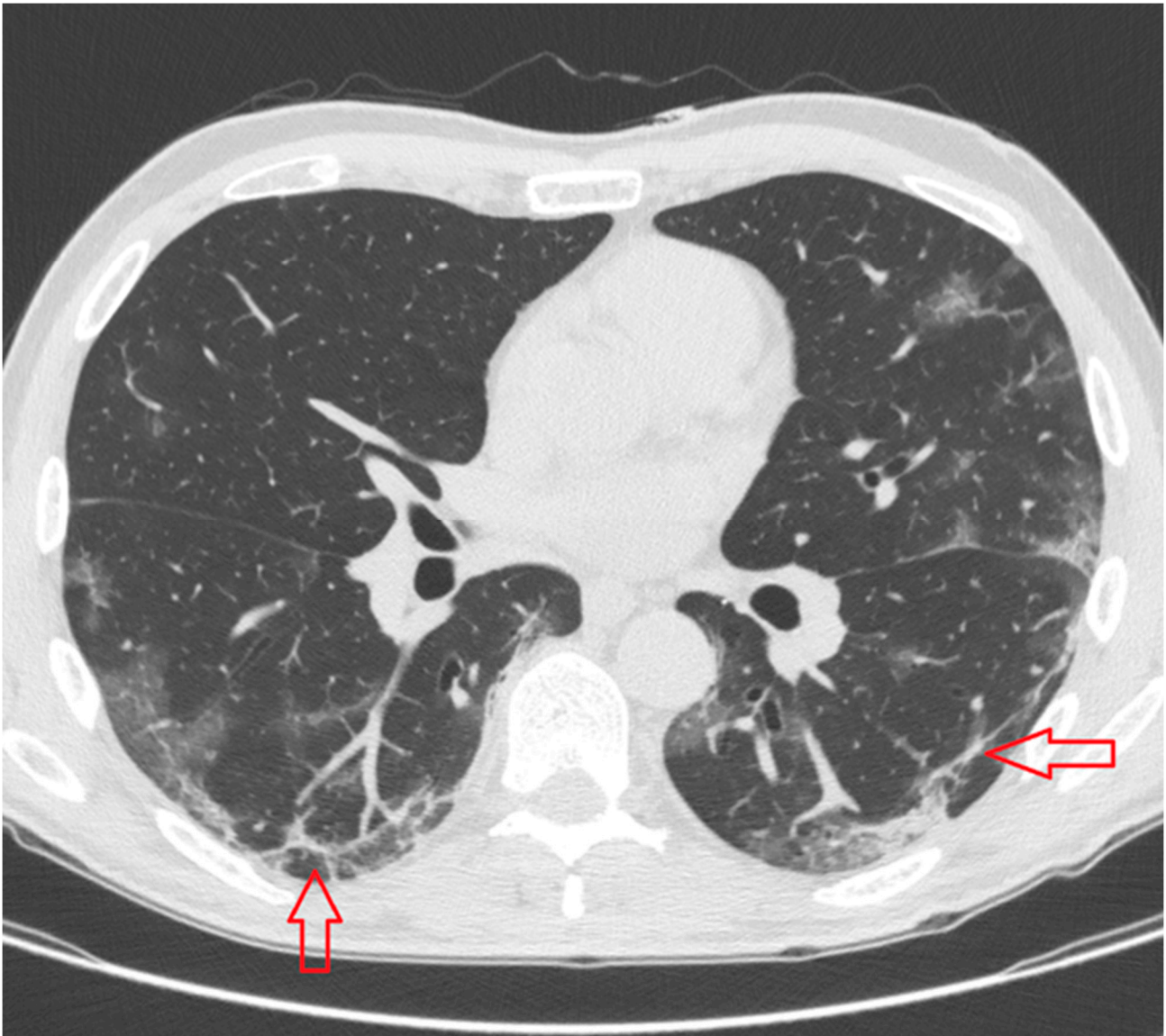
Figure 4. Axial image of HRCT of lungs in a 68-year-old man with PCR-confirmed COVID-19 pneumonia showing bilateral curvilinear subpleural opacity (red arrows).

- Tree in bud: centrilobular branching structures reflecting a spectrum of endo- and peribronchiolar changes;
- Honeycombing: clustered cystic air spaces, typically with comparable diameters in the order of 3–10 mm, subpleural and with well-defined walls, for example, in fibrotic lung;
- Vascular enlargement sign: dilatation of pulmonary vessels around, within, or near a parenchymatous change (Figure 5) [9];
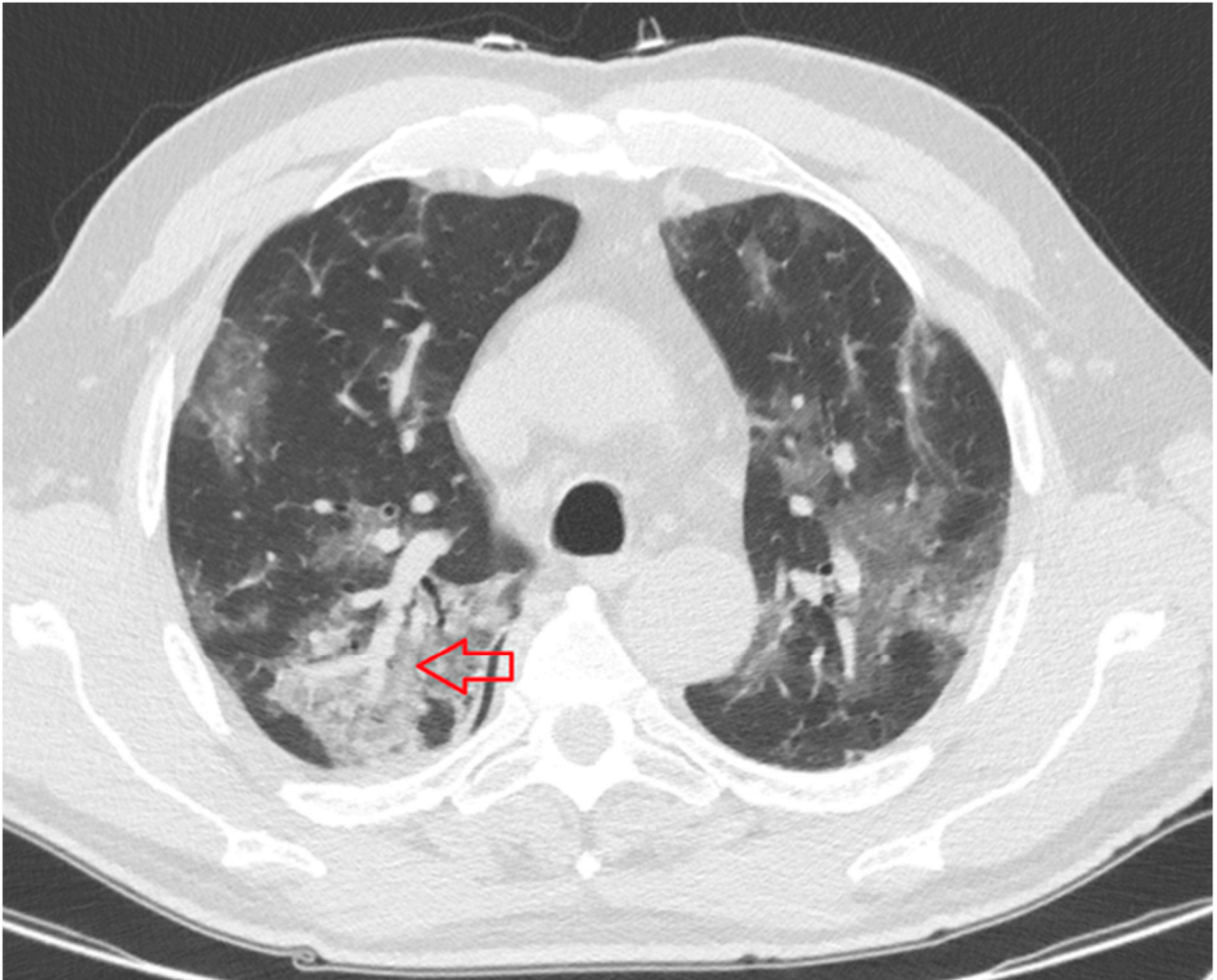
Figure 5. Axial image of HRCT of lungs in a 57-year-old man with PCR-confirmed COVID-19 pneumonia showing a dilated pulmonary vein within an area of parenchymal consolidation (red arrow).

- Pulmonary nodule: roundish opacity up to 3 cm in diameter;
- Cavitation: gas-filled space within the pulmonary consolidation or nodule;
- Smooth interlobular septal thickening: a disease affecting one of the components of the septa that may be responsible for the thickening, making the septa visible, e.g., pulmonary oedema;
- Pleural effusion;
- Mediastinal lymphadenopathy: presence of several lymph nodes with a diameter of at least 10 mm [10].

The presence and number of lung abnormalities in each bronchopulmonary segment were recorded in a database for statistical analysis and to create a formal scoring system. All CT scans that did not show any of these signs were considered negative. If more than one CT scan was performed in the same treatment episode, only the scan closest to the ED recording was reviewed. A random 30% of the sample was used to develop the HRCT score, and all the population was used to validate the score.
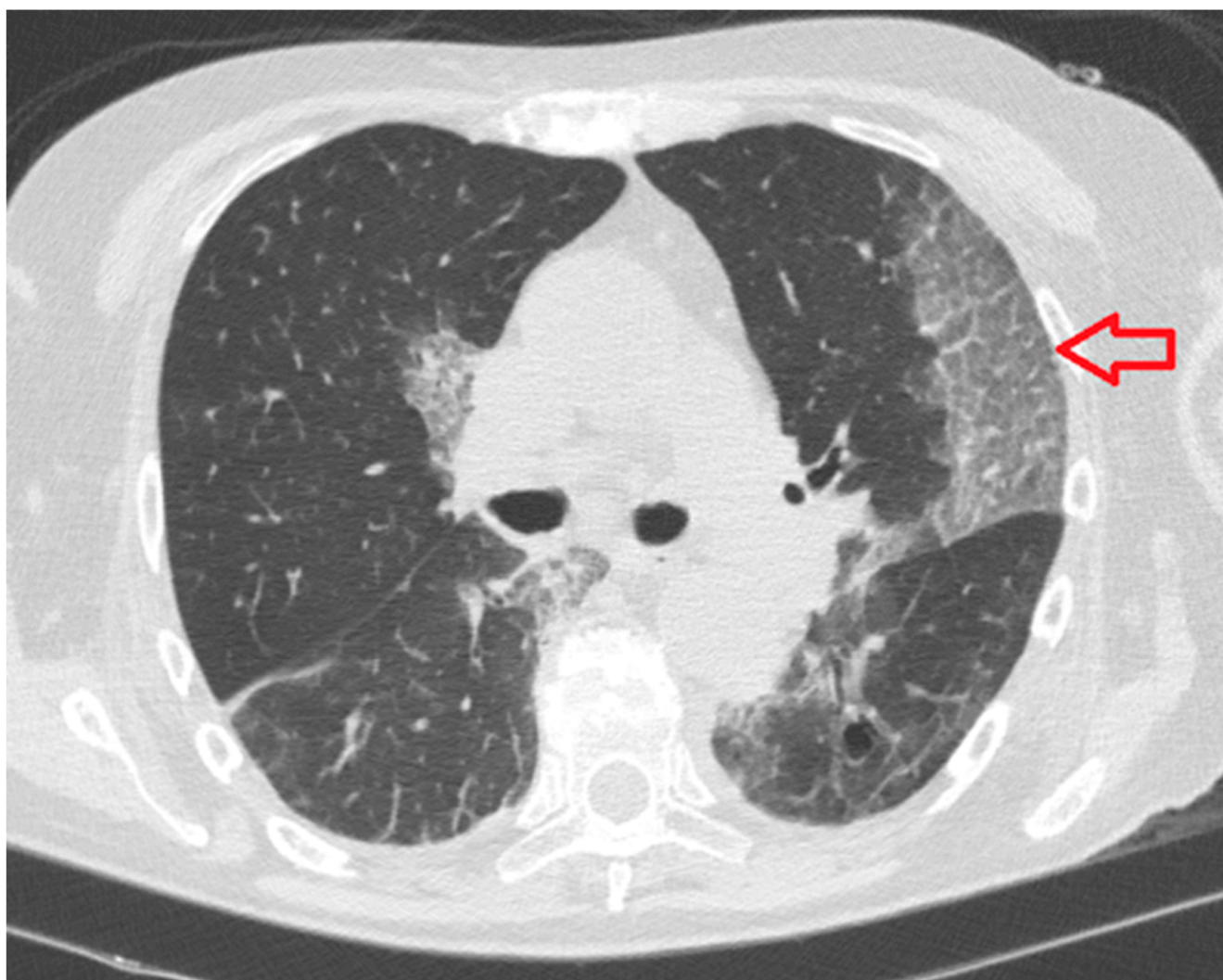
Figure 6. Axial image of HRCT of lungs in a 69-year-old woman with PCR-confirmed COVID-19 pneumonia showing bilateral areas of ground glass opacities with superimposed thickening of interlobular septa (crazy paving), particularly evident in the left upper lobe (red arrow).

2.2. Clinical and Laboratory Data

Clinical data at admission were retrospectively extracted from the hospital informatics system and blinded to HRCT. According to the local SARS-CoV-2 diagnostic protocol, the standard diagnosis was reverse transcription polymerase chain reaction (RT-PCR) to detect SARS-CoV-2 RNA in the nasopharyngeal swab. In case of a negative smear and a clinical high suspicion of COVID-19, the smear was repeated at least three times. Patients with repeated negative smears, low clinical suspicion, and another underlying cause of respiratory distress were classified as COVID-19-negative, and patients with high suspicion of COVID-19 underwent alveolar broncolavage and serological examination before being classified as negative. In case the specific agent was not determined, the patient was identified as a non-specific pneumonia. For this study, COVID-19 diagnosis was determined according to the final diagnosis of hospital discharge. All data were retrospectively extracted from the patients' electronic medical records by an experienced emergency medicine physician and four residents with at least 3 years of experience in the emergency department.

2.3. Statistical Evaluation

Normally distributed data are expressed as mean and standard deviation (SD) and were compared using the *t*-test for independent samples. Non-normally distributed data were reported as median and interquartile range (IQR) and compared using the Mann–Whitney U-test. Categorical data were reported as absolute numbers and percentages, and Pearson's chi-square test was used to compare categorical dependent variables between at least two independent groups. Univariate analyses were performed to identify predictors of SARS-CoV-2-positive smears. A random 30% of the sample was used to develop the HRCT score, and all the population was used to validate the score. Predictors from univariate analysis were included in the multivariate analysis to create a final model that included only independent predictors. The final score was created by assigning a few points to each item that corresponded to the odds ratios. Missing data that were not required to calculate the score were replaced by a regressive multiple imputation analysis [11]. The discriminatory ability of the score was tested using the receiver operator characteristic (ROC) curve. The optimal threshold for best discrimination was determined using the highest Youden index. The calibration of the developed model was assessed using the Hosmer–Lemeshow test [12]. Analysis of the linear regression model of the score was performed to check for multicollinearity via a variance inflation factor (VIF) assessment. Statistical analyses were performed using SPSS v.25 (Apache Software Foundation, Chicago, IL, USA) and MedCalc version 17.6 (MedCalc Statistical Software version 17.6 (MedCalc Software Ltd., Ostend, Belgium).

3. Results

A total of 1153 patients were included in the study. Of these, 457 (39.6%) tested positive for SARS-CoV-2. A nasopharyngeal swab was repeated at least once in 327 patients (28.36% of total): once in 229 patients (70% of repeated swabs), twice in 63 patients (19.3% of cases), and more than twice in 26 patients (7.9%). Finally, a positive nasopharyngeal swab for SARS-CoV-2 was found in 58 of the 315 patients (18.4%). COVID-19 patients were younger than those without COVID-19 (64.8 years versus 71.8 years, $p < 0.001$) and were more likely to present with fever and cough in the ED. These patients had higher systolic blood pressure, body temperature, and pH values; lower pCO2, pO2, and PF values; and lower leukocyte, neutrophil, lymphocyte, and platelet counts than patients without COVID-19. COVID-19 patients had significantly higher levels of interleukin 6 (IL-6), fibrinogen, lactate dehydrogenase (LDH), and ferritin and a significantly higher rate of in-hospital death (16.7% vs. 9.1%, *p*-value 0.001) (see Table 1). The percentage of patients with negative HRCT was lower in those with confirmed SARS-CoV-2 infection (10% vs. 44.2%, $p < 0.001$); 89.9% of COVID-19 patients had at least one sign of lung disease, significantly higher than non-COVID-19 patients (55.8% of cases, $p < 0.001$) (Table 2). Regarding radiological signs, in COVID-19 patients HRCT showed GGOs in a higher percentage of cases (74.8 vs. 36.1, $p < 0.001$) and a higher number of lung segments with GGO (7.79 vs. 3.69, $p < 0.001$). Linear consolidations, crazy paving pattern, honeycombing, and vascular ectasia were significantly more common in these patients, while consolidations with and without air bronchograms, tree-in-bud, edematous thickening of the interlobular septa, and pleural effusions were more common in patients without SARS-CoV-2 infection. The number of segments with GGO, the number of segments with linear consolidations, and the presence of crazy patterns and/or vascular ectasia in each segment were identified as independent predictors of SARS-CoV-2 in univariate and multivariate analysis. Therefore, they were included in the final scores. The final HRCT score was calculated for all patients, as shown in Table 3. The median HRCT score was 14.4, with a significantly higher value in patients with SARS-CoV-2 (15.67 vs. 8.82 *p*-value < 0.001) (Table 2). Considering only patients who underwent repeated swabs, those who tested positive for SARS-CoV-2 infection had a significantly higher HRCT score (median 6.01 (IQR 0–11.81) versus 0 (IQR 0–3.54), $p < 0.001$). The HRCT score had high accuracy for SARS-CoV-2 infection, with an AUROC score of 0.83 (95% CI 0.8–0.86) (see Figure 7). The best cut-off was determined to be an HRCT score ≥ 4,

with 72.2% sensitivity (95% CI 67.9–76.3), 86.6% specificity (95% CI 83.9–89.1), 78% PPV (95% CI 73.8–81.9), and 83% NPV (95% CI 79.7–85.3). HRCT score of 0 had a sensitivity of 80% (95% CI 76.1–83.6) and a negative likelihood ratio of 0.26 (95% CI 0.2–0.3), while HRCT score > 10 had a specificity of 95.74 (95% CI 94–97.1) and a positive likelihood ratio of 9.17 (95% CI 8.2–10.3) (Table 4). In the linear regression model analysis, each item included in the HRCT score had a variance inflation factor (VIF) of <1.12, excluding multicollinearity.

Table 1. Characteristics of included patients.

	Patients Included, 1153	SARS-CoV-2-Negative, 696 (60.4%)	SARS-CoV-2-Positive, 457 (39.6%)	*p*-Value
Age, years, media (SD)	67.06 (18.35)	71.8 (17.4)	64.83 (11)	<0.001
Male, N (%)	649 (56.3)	379 (54.5)	270 (59.2)	0.11
Fever, N (%)	764 (66.9)	389 (56.6)	375 (82.8)	<0.001
Cough, N (%)	429 (37.6)	211 (30.7)	218 (48.1)	<0.001
Dyspnea, N (%)	423 (37.2)	252 (36.6)	173 (38.1)	0.8
Diarrhea, N (%)	143 (12.5)	88 (12.8)	55 (12.1)	0.53
HR, ppm, media (SD)	93.38 (18.8)	91 (20)	95 (16)	0.35
RR, app, media (SD)	19.55 (7.2)	18.44 (7)	20.44 (4.5)	0.26
SBP, mmHg, media (SD)	128.1 (24)	131 (27)	124 (18)	<0.001
DBP, mmHg, media (SD)	74.71 (13.9)	75 (14)	74.4 (10)	0.12
Body temperature in C, median (IQR)	36.87 (1)	36.47 (1)	37.23 (2)	<0.001
pH, median (IQR)	7.47 (0.07)	7.44 (0)	7.49 (0)	<0.001
pCO2, mmHg, median (IQR)	35.5 (8)	36.5 (9)	33 (6)	<0.001
pO2, mmHg, median (IQR)	65 (21)	72 (22)	63 (19)	<0.001
sO2, %, median (IQR)	96 (3)	97 (3)	94.8 (3)	<0.001
P/F ratio, media (SD)	302.5 (89)	307 (108)	295 (66)	<0.001
Leukocytes, N/mL, median (IQR)	8.34 (6)	9.56 (9.6)	6.59 (4)	<0.001
Neutrophils, N/mL, median (IQR)	6.21 (5)	8.89 (10)	5.36 (4)	<0.001
Lymphocytes, N/mL, median (IQR)	1.23 (1)	1.64 (1.48)	0.87 (0.51)	<0.001
Eosinophils, N/mL, median (IQR)	0.02 (0)	0.025 (0.14)	0.0 (0.1)	<0.001
Platelets, * 1000/mL, median (IQR)	223 (106)	221 (139)	236 (59)	<0.001
IL-6, ng/dL, median (IQR)	36 (57)	28 (92)	40 (51)	0.04
Fibrinogen, mg/dL, median (SD)	497 (148)	440 (165)	486 (129)	0.005
LDH, mg/dL, median (IQR)	263 (208)	206 (102)	262 (141)	<0.001
C-reactive protein, mg/mL, median (SD)	11 (14)	10.5 (8.23)	12.25 (7.31)	0.22
Ferritins, mg/mL median (IQR)	252 (338)	129 (224)	334 (534)	<0.001
Procalcitonin, ng/mL, median (IQR)	0,1 (0)	0.1 (0)	0.1 (0)	0.08
d-Dimer, FEU/mL median (IQR)	0.87 (1)	0.99 (3)	0.81 (1)	0.35
No in-hospital therapy amongst selected, N (%)	138 (12.8)	129 (20.2)	9 (2.1)	<0.001
Hydroxychloroquine, N (%)	540 (50.7)	161 (25.6)	379 (86.9)	<0.001
Antibiotic, N (%)	786 (73.8)	396 (63)	390 (89.4)	<0.001
Tocilizumab, N (%)	96 (9.1)	8 (1.3)	88 (20.5)	<0.001
Antivirals, N (%)	61 (5.8)	15 (2.4)	46 (10.8)	<0.001
Cortisone, N (%)	272 (26.1)	102 (16.5)	170 (40.3)	<0.001
LMWH, N (%)	602 (58.4)	274 (45.1)	328 (77.9)	<0.001
In-hospital dead patients, N (%)	130 (12.1)	60 (9.1)	70 (16.7)	<0.001

Note: *: best cut-off.

Table 2. HRCT characteristics of included patients.

	Patients Included, 1153	SARS-CoV-2-Negative, 696 (60.4%)	SARS-CoV-2-Positive, 457 (39.6%)	*p*-Value
Negative HRCT, N (%)	357 (30.9)	306 (44.2)	46 (10.1)	<0.001
Positive for any sign HRCT, N (%)	796 (69.1)	387 (55.8)	409 (89.9)	< 0.001
HRCT score, median (SD)	14.41 (5.34)	8.82 (4.68)	15.67 (4.66)	<0.001
GGO, N (%)	446 (56)	140 (36.1)	306 (74.8)	<0.001
Number of segments with GGO, median (SD)	7.04 (3.7)	3.69 (2.1)	7.79 (3.57)	<0.001
Consolidations with air bronchogram, N (%)	261 (32.8)	154 (39.8)	107 (26.2)	<0.001
Consolidations without air bronchogram, N (%)	219 (27.5)	121 (31.3)	98 (24)	0.031
Linear consolidations, N (%)	106 (13.4)	33 (8.5)	73 (17.9)	<0.001
Number of segment with linear consolidations, median (SD)	3.28 (1.93)	2 (1.9)	3.46 (1.85)	0.032
Solitary nodules, N (%)	106 (13.4)	27 (3.6)	20 (4.4)	0.277
Crazy paving, N (%)	196 (24.7)	35 (9.1)	161 (39.4)	<0.001
Tree in bud, N (%)	69 (8.7)	59 (15.3)	10 (2.5)	<0.001
Honeycombing, N (%)	20 (2.5)	16 (4.2)	4 (1)	0.004
Vascular ectasia, N (%)	70 (11.3)	9 (2.9)	61 (19.4)	<0.001
Cavitation, N (%)	2 (0.3)	2 (0.6)	0 (0)	0.164
Edematous thickening of the interlobular septa, right lung, N (%)	52 (8.3)	45 (14.5)	7 (2.2)	<0.001
Edematous thickening of the interlobular septa, left lung, N (%)	54 (8.7)	47 (15.2)	7 (2.2)	<0.001
Focal heteroplastic lesions, N (%)	16 (2.6)	14 (4.5)	2 (0.6)	0.003
Lymphadenopathy, N (%)	75 (12)	44 (14.2)	31(9.9)	0.19
Pleural effusion, right lung, N (%)	138 (22.2)	110 (35.5)	28 (8.9)	<0.001
Pleural effusion, left lung, N (%)	135 (21.7)	104 (33.7)	31 (9.9)	<0.001

Table 3. HRCT score calculator.

|	Point	Total
Number of segments with GGO	1 point per segment	
Number of segments with linear consolidations	1 point per segment	
Presence of crazy paving in any segment	6 points	
Presence of vascular ectasia in any segment	2.5 points	
HRCT score, total:	--------------	
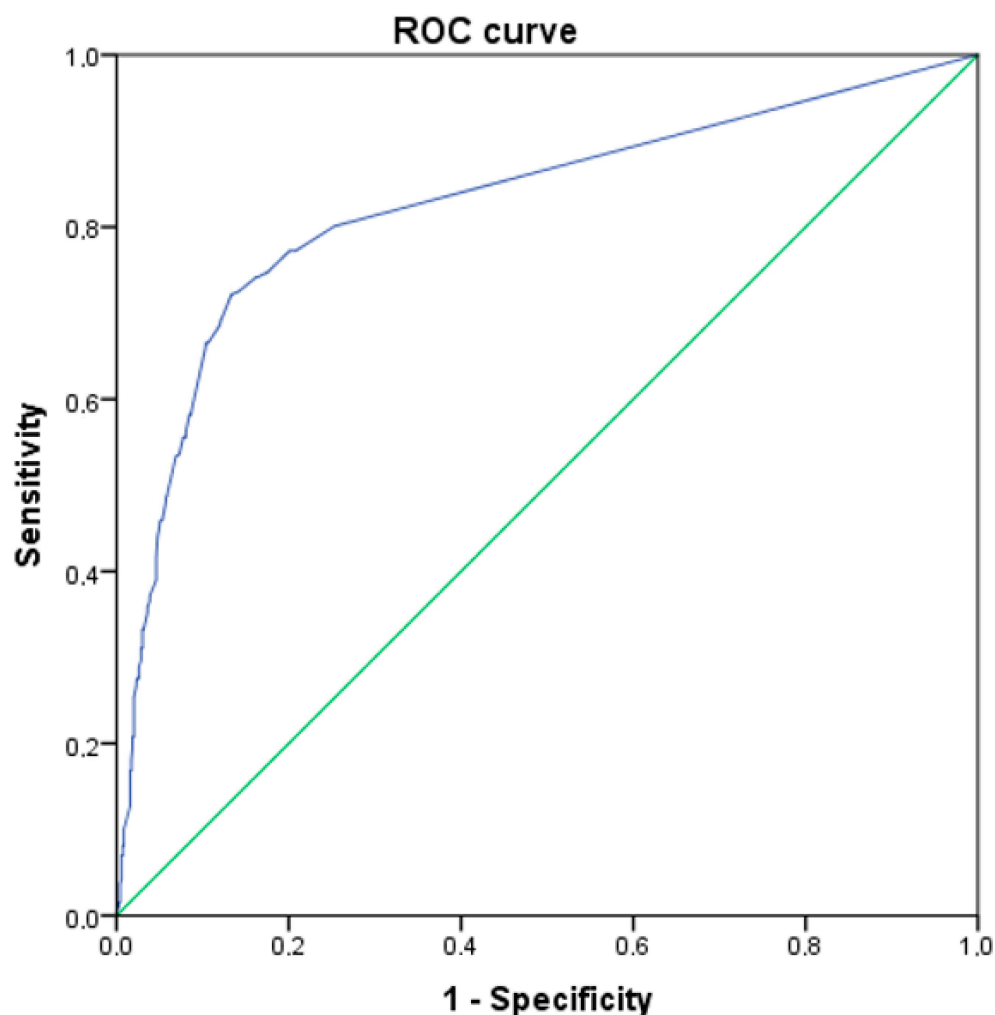
Figure 7. AUROC of the HRCT score. AUROC = 0.826, 95% CI 0.8–0.86.

Table 4. Diagnostic accuracy of the HRCT score.

HRCT Score	Sensitivity	95% CI	Specificity	95% CI	+LR	95% CI	−LR	95% CI
>0	80.09	76.1–83.7	74.71	71.3–77.9	3.17	3–3.4	0.27	0.2–0.3
≥4 *	72.2	67.9–76.3	86.6	83.9–89.1	5.74	5.4–6.1	0.36	0.3–0.5
>10	38.95	34.5–43.6	95.4	93.6–96.8	8.47	7.5–9.5	0.64	0.5–0.9
>15	20.35	16.8–24.3	98.13	96.8–99	10.9	9.1–13.1	0.81	0.5–1.4

Note: *: best cut-off.

4. Discussion

Even in the early stages of the COVID-19 pandemic, it quickly became clear that timely detection of the disease is of paramount importance for individual treatment and public health. In the context of this epidemiological storm, which has put enormous pressure on health facilities worldwide, HRCT of the chest has played a central role in the diagnosis of COVID-19 mainly because of its greater availability than the standard RT-PCR test and the large amount of information it can provide about the condition of the lungs. Early reports also attested to HRCT's higher sensitivity for COVID-19 pneumonia and its ability to anticipate the diagnosis at presentation compared to the RT-PCR test [13–15].

However, at the onset of the pandemic, most radiological societies discouraged the use of CT in the initial evaluation of patients with suspected pneumonia [16], recommending that it should be limited to patients with moderate-to-severe clinical features and a high

pretest probability [17,18]. In contrast to its diagnostic efficacy, HRCT has several disadvantages, including its inhomogeneous distribution in different facilities, the use of ionizing radiation, the additional staff required to mobilize and clean patients, the risk of queue formation in crowded facilities (e.g., emergency departments), and last but not least the commonality of some features of COVID-19 with other viral pneumonias or non-infectious etiologies [19–22].

According to the results of this study, the number of segments with GGO, the number of segments with linear consolidations, the presence of a crazy paving pattern in a segment, and the presence of vascular ectasia in a segment correlate independently with the diagnosis of COVID-19. The resulting HRCT score (1 point for each segment with GGO, 1 point for each segment with linear consolidation, 6 points for the presence of crazy paving patterns, and 2.5 points for the presence of vascular ectasia) showed high accuracy in predicting COVID-19, with an AUROC value of 0.826 (95% CI 0.8–0.86). While an HRCT score of 0 has low sensitivity and cannot be used to rule out SARS-CoV-2 infection, an HRCT score > 10 is highly specific for COVID-19, with a +LR of 11 for HRCT score > 15 almost confirming the diagnosis of COVID-19. This confirms that imaging techniques are not able to rule out SARS-CoV-2 infection and, due to their limited sensitivity in asymptomatic patients, are of limited use in determining whether a patient at risk of infection should be isolated [23]. A few studies [13,15] have directly compared the results of chest examination CT with RT-PCR as a reference and found that CT has a high sensitivity (97% to 98%) but a low-to-moderate specificity (25% to 56%) and an accuracy of 68–72% for the diagnosis of COVID-19 pneumonia, with a positive predictive value (PPV) and negative predictive value (NPV) of 65% and 83%, respectively [1]. A 2021, Cochrane meta-analysis on COVID-19-related imaging gave a pooled sensitivity of 87.9 (95% CI 84.6 to 90.6) and a pooled specificity of 80% (95% CI 74.9 to 84.3) for chest CT [5], which is not significantly different from the results of Khatami et al., who reported an overall sensitivity, specificity, positive predictive value, and negative predictive value of CT compared with RT-PCR of 87% (95% CI 85–90%), 46% (95% CI 29–63%), 69% (95% CI 56–72%), and 89% (95% CI 82–96%), respectively [23]. An increase in CT specificity has also been achieved by combining two or more statistically significant CT signs (up to 99% for GGOs with crazy patches and bilateral distribution) [24] or by using formal scoring systems and standardized assessments [16,25,26].

In most published studies [27,28], HCRTs are considered positive depending on the presence of some signs considered typical of SARS-CoV-2 pneumonia, such as GGOs, crazy paving, multifocal organizing pneumonia with peripheral distribution, and predominant lower-lobe involvement, especially in advanced disease. The radiological pattern of pulmonary abnormalities is dynamic and variable in relation to the stage of pneumonia [4,29,30], making it difficult to establish a definite relationship between each radiological configuration and the diagnosis of the disease. Several studies have proposed scores based on semi-quantitative or qualitative assessments of HRCT changes in patients with suspected COVID-19 pneumonia, aimed at the diagnosis or staging of the disease [4,29–31].

In March 2020, the Radiological Society of North America (RSNA) launched an initiative to standardize COVID-19 reporting [16]. The British Society of Thoracic Imaging (BSTI) proposed a similar initiative but also added a descriptor for disease severity that differentiates between mild and moderate/severe disease, although these efforts are not based on evidence of patient outcomes [32]. The COVID-19 Reporting and Data System (CO-RADS) is another initiative to standardize HRCT reading and reporting, which was published in mid-March 2020 [25] and developed on the CTs of 105 suspected COVID-19 patients, demonstrating high accuracy (AUROC 0.91, 95% CI 0.85–0.97) but low interobserver agreement (Fleiss' kappa 0.47, 95% CI 0.45–0.47). Moreover, while all these efforts have the merit of attempting to standardize the approach to CT images suggestive of COVID-19 in the early stages of the pandemic, they are based on a qualitative assessment of images that are considered typical without any measurable objective assessment. According to the results of this study, the number of segments with GGO, the number of segments with linear consolidations, and the presence of crazy paving and vascular ectasia in each

segment were independent predictors of COVID-19 and were included in a five-level HRCT score. Both ground glass opacity and crazy paving are commonly associated with various diseases [33], the latter with ARDS, tumors, lymphangitis carcinomatosis, radiation pneumonitis, sarcoidosis, alveolar proteinosis, graft-versus-host disease, and rarely with acute pulmonary oedema, bacterial, fungal, and viral pneumonia [34], all having a low prevalence in the general population. Therefore, knowledge of the prevalence of the diseases in the population, together with correct clinical suspicion, can help to make these signs more specific. Previous studies have shown that the presence of bilateral bronchial wall thickening, crazy paving, linear consolidations and GGO can predict a severe form of COVID-19 [35]. In addition, several scores have been proposed to predict the severity of COVID-19, which have high accuracy [3,25,36]. However, to the best of our knowledge, few scores have been developed specifically for assessing the likelihood of SARS-CoV-2 infection. In this light, the role of artificial intelligence (AI) promises to be of paramount importance. Despite the need for a further, proper development and clinical evaluation of AI before its use in clinical practice, AI has demonstrated not only to be able to predict the risk of deterioration to critical illness based on CT images and clinical data [37] but also to predict the likelihood of COVID-19 based on the CO-RADS-standardized CT scoring systems with high accuracy [38] comparable to the results of HRCT score.

The HRCT score gives one point for each segment with GGOs and one point for each segment with linear consolidation. The extent of these pathological signs in the lung is considered more significant than their detection without adequate quantification due to their low specificity. The HRCT score ranged from 0 to 32.5 points, with 0 representing no abnormalities and 32.5 representing GGOs and linear consolidation in all lung segments, crazy paving, and vascular abnormalities (see Table 3), being able to combine the extent of lung involvement, a significant predictor of COVID-19, and the presence of specific lung abnormalities in a single score [37,38].

This score provides a clear and standardized method for describing and measuring pulmonary involvement based on significant abnormalities. It objectively assesses lung involvement in COVID-19 and is quick, easy to use, and suitable for better integration of HRCT into the diagnostic pathway of COVID-19 pneumonia in the emergency department.

Limitation

This study has some limitations. First, it was monocentric, which may have affected the diagnostic accuracy of HRCT and sensitivity of detection methods for SARS-CoV-2 infection. Second, each HRCT was retrospectively evaluated individually by radiologists, and inter-rater variability was not calculated using the score. Third, we included only patients admitted to the emergency department during the first wave of the pandemic, whereas protection by vaccination and the emergence of new viral variants may alter the radiological aspects of SARS-CoV-2 infection [39]. Fourth, we did not report the prognostic accuracy of the score in terms of the risk of clinical deterioration and mortality, which could also be influenced by the high impact of newly developed therapies and vaccinations [40]. In addition, we did not calculate the formal sample size because there are no generally accepted methods for estimating the sample size in risk-prediction models. According to the recommended "rule of ten events per predictor" in multivariable logistic regression analysis, this study contains many more events than required for the four-point model developed [41].

5. Conclusions

The SARS-CoV-2 infection has put pressure on health systems worldwide. In recent years, the approach to the disease in terms of prevention, diagnosis, and treatment has completely changed; however, there are still many areas in which we can improve our knowledge. The extensive use of chest CT has provided valuable insight to the diagnosis and prognosis of COVID-19. Despite the limited specificity of an individual radiological sign, the HRCT score has demonstrated a high level of diagnostic accuracy for COVID-19.

This score incorporates the most predictive radiological signs and their distribution into a single, straightforward, quantitative measure. It has been found to significantly impact the post-test probability of SARS-CoV-2 infection in a large cohort of patients with suspected COVID-19 who were enrolled in the emergency department.

Author Contributions: Conceptualization, S.S., M.D.S. and P.O.; data curation, L.C. (Leonardo Catalano), R.M., L.M., E.S., L.C. (Laura Colì), V.M., C.R. and B.S.; formal analysis, D.A. and M.D.S.; methodology, D.A. and M.D.S.; project administration, P.O.; resources, M.I.; software, D.A.; supervision, S.S. and A.B.; validation, P.O.; visualization, M.D.S.; writing—original draft, S.S., G.F. and M.D.S.; writing—review and editing, M.I. and P.O. All authors have read and agreed to the published version of the manuscript.

Institutional Review Board Statement: The study was conducted in accordance with the Declaration of Helsinki and approved by the Ethics Committee of Area Vasta Emilia Centro (AVEC) rif. CE AVEC n. 58/2021/OSS/AUSLBO, 04 January 2021.

Informed Consent Statement: Patient consent was waived due to the retrospective nature of the study.

Data Availability Statement: Data are available on request.

Conflicts of Interest: The authors declare no conflict of interest.

References

1. Available online: https://news.un.org/en/story/2023/05/1136367 (accessed on 11 September 2023).
2. Arevalo-Rodriguez, I.; Buitrago-Garcia, D.; Simancas-Racines, D.; Zambrano-Achig, P.; Del Campo, R.; Ciapponi, A.; Sued, O.; Martinez-García, L.; Rutjes, A.W.; Low, N.; et al. False-negative results of initial RT-PCR assays for COVID-19: A systematic review. *PLoS ONE* **2020**, *15*, e0242958. [CrossRef]
3. Elmokadem, A.H.; Mounir, A.M.; Ramadan, Z.A.; Elsedeiq, M.; Saleh, G.A. Comparison of chest CT severity scoring systems for COVID-19. *Eur. Radiol.* **2022**, *32*, 3501–3512. [CrossRef]
4. Pan, F.; Ye, T.; Sun, P.; Gui, S.; Liang, B.; Li, L.; Zheng, D.; Wang, J.; Hesketh, R.L.; Yang, L.; et al. Time Course of Lung Changes at Chest CT during Recovery from Coronavirus Disease 2019 (COVID-19). *Radiology* **2020**, *295*, 715–721. [CrossRef]
5. Islam, N.; Ebrahimzadeh, S.; Salameh, J.-P.; Kazi, S.; Fabiano, N.; Treanor, L.; Absi, M.; Hallgrimson, Z.; Leeflang, M.M.G.; Hooft, L.; et al. Thoracic imaging tests for the diagnosis of COVID-19. *Cochrane Database Syst. Rev.* **2021**, *3*, CD013639. [CrossRef]
6. Bossuyt, P.M.; Reitsma, J.B.; Bruns, D.E.; Gatsonis, C.A.; Glasziou, P.P.; Irwig, L.; Lijmer, J.G.; Moher, D.; Rennie, D.; de Vet, H.C.W.; et al. STARD 2015: An updated list of essential items for reporting diagnostic accuracy studies. *BMJ* **2015**, *351*, h5527. [CrossRef]
7. Collins, G.S.; Reitsma, J.B.; Altman, D.G.; Moons, K.G. Transparent reporting of a multivariable prediction model for individual prognosis or diagnosis (TRIPOD): The TRIPOD statement. *BMJ* **2015**, *350*, g7594. [CrossRef] [PubMed]
8. Hansell, D.M.; Bankier, A.A.; MacMahon, H.; McLoud, T.C.; Müller, N.L.; Remy, J. Fleischner Society: Glossary of terms for thoracic imaging. *Radiology* **2008**, *246*, 697–722. [CrossRef]
9. Ye, Z.; Zhang, Y.; Wang, Y.; Huang, Z.; Song, B. Chest CT manifestations of new coronavirus disease 2019 (COVID-19): A pictorial review. *Eur. Radiol.* **2020**, *30*, 4381–4389. [CrossRef] [PubMed]
10. Iyer, H.; Anand, A.; Icon, P.B.S.; Gupta, K.; Naranje, P.; Damle, N.; Icon, S.M.; Madan, N.K.; Icon, A.M.; Hadda, V.; et al. Mediastinal lymphadenopathy: A practical approach. *Expert Rev. Respir. Med.* **2021**, *15*, 1317–1334. [CrossRef]
11. Yu, L.; Liu, L.; Peace, K.E. Regression multiple imputation for missing data analysis. *Stat. Methods Med. Res.* **2020**, *29*, 2647–2664. [CrossRef] [PubMed]
12. Hosmer, D.W.; Hosmer, T.; Le Cessie, S.; Lemeshow, S. A comparison of goodness-of-fit tests for the logistic regression model. *Stat. Med.* **1997**, *16*, 965–980. [CrossRef]
13. Ai, T.; Yang, Z.; Hou, H.; Zhan, C.; Chen, C.; Lv, W.; Tao, Q.; Sun, Z.; Xia, L. Correlation of Chest CT and RT-PCR Testing for Coronavirus Disease 2019 (COVID-19) in China: A Report of 1014 Cases. *Radiology* **2020**, *296*, E32–E40. [CrossRef] [PubMed]
14. Fang, Y.; Zhang, H.; Xie, J.; Lin, M.; Ying, L.; Pang, P.; Ji, W. Sensitivity of Chest CT for COVID-19: Comparison to RT-PCR. *Radiology* **2020**, *296*, E115–E117. [CrossRef] [PubMed]
15. Caruso, D.; Zerunian, M.; Polici, M.; Pucciarelli, F.; Polidori, T.; Rucci, C.; Guido, G.; Bracci, B.; De Dominicis, C.; Laghi, A. Chest CT Features of COVID-19 in Rome, Italy. *Radiology* **2020**, *296*, E79–E85. [CrossRef] [PubMed]

16. Simpson, S.; Kay, F.U.; Abbara, S.; Bhalla, S.; Chung, J.H.; Chung, M.; Henry, T.S.; Kanne, J.P.; Kligerman, S.; Ko, J.P.; et al. Radiological Society of North America Expert Consensus Document on Reporting Chest CT Findings Related to COVID-19: Endorsed by the Society of Thoracic Radiology, the American College of Radiology, and RSNA. *Radiol. Cardiothorac. Imaging* **2020**, *2*, e200152. [CrossRef] [PubMed]

17. Rubin, G.D.; Ryerson, C.J.; Haramati, L.B.; Sverzellati, N.; Kanne, J.P.; Raoof, S.; Schluger, N.W.; Volpi, A.; Yim, J.-J.; Martin, I.B.K.; et al. The Role of Chest Imaging in Patient Management during the COVID-19 Pandemic: A Multinational Consensus Statement from the Fleischner Society. *Radiology* **2020**, *296*, 172–180. [CrossRef]

18. Available online: https://www.acr.org/Advocacy-and-Economics/ACR-Position-Statements/Recommendations-for-Chest-Radiography-and-CT-for-Suspected-COVID19-Infection (accessed on 11 September 2023).

19. Guarnera, A.; Santini, E.; Podda, P. Idiopathic Interstitial Pneumonias and COVID-19 Pneumonia: Review of the Main Radiological Features and Differential Diagnosis. *Tomography* **2021**, *7*, 397–411. [CrossRef]

20. Koo, H.J.; Lim, S.; Choe, J.; Choi, S.H.; Sung, H.; Do, K.H. Radiographic and CT Features of Viral Pneumonia. *Radiographics* **2018**, *38*, 719–739. [CrossRef]

21. Li, Y.; Xia, L. Coronavirus Disease 2019 (COVID-19): Role of Chest CT in Diagnosis and Management. *AJR Am. J. Roentgenol.* **2020**, *214*, 1280–1286. [CrossRef]

22. Bai, H.X.; Hsieh, B.; Xiong, Z.; Halsey, K.; Choi, J.W.; Tran, T.M.L.; Pan, I.; Shi, L.-B.; Wang, D.-C.; Mei, J.; et al. Performance of Radiologists in Differentiating COVID-19 from Non-COVID-19 Viral Pneumonia at Chest CT. *Radiology* **2020**, *296*, E46–E54. [CrossRef]

23. Khatami, F.; Saatchi, M.; Zadeh, S.S.T.; Aghamir, Z.S.; Shabestari, A.N.; Reis, L.O.; Aghamir, S.M.K. A meta-analysis of accuracy and sensitivity of chest CT and RT-PCR in COVID-19 diagnosis. *Sci. Rep.* **2020**, *10*, 22402. [CrossRef] [PubMed]

24. Miao, C.; Jin, M.; Miao, L.; Yang, X.; Huang, P.; Xiong, H.; Huang, P.; Zhao, Q.; Du, J.; Hong, J. Early chest computed tomography to diagnose COVID-19 from suspected patients: A multicenter retrospective study. *Am. J. Emerg. Med.* **2021**, *44*, 346–351. [CrossRef]

25. Prokop, M.; van Everdingen, W.; van Rees Vellinga, T.; van Ufford, H.Q.; Stöger, L.; Beenen, L.; Geurts, B.; Gietema, H.; Krdzalic, J.; Schaefer-Prokop, C.; et al. CO-RADS: A Categorical CT Assessment Scheme for Patients Suspected of Having COVID-19-Definition and Evaluation. *Radiology* **2020**, *296*, E97–E104. [CrossRef] [PubMed]

26. Available online: https://www.bsti.org.uk/covid-19-resources/covid-19-bsti-reporting-templates/ (accessed on 11 September 2023).

27. Calvi, C.; Ferreira, F.F.; Lyrio, L.; de Melo Baptista, R.; Zanoni, B.B.; Junger, Y.O.; Barros, W.H.; Volpato, R.; Júnior, L.M.; Júnior, M.R. COVID-19 findings in chest computed tomography. *Rev. Assoc. Med. Bras.* **2021**, *67*, 1409–1414. [CrossRef] [PubMed]

28. Zheng, Y.; Wang, L.; Ben, S. Meta-analysis of chest CT features of patients with COVID-19 pneumonia. *J. Med. Virol.* **2021**, *93*, 241–249. [CrossRef]

29. Chung, M.; Bernheim, A.; Mei, X.; Zhang, N.; Huang, M.; Zeng, X.; Cui, J.; Xu, W.; Yang, Y.; Fayad, Z.A.; et al. CT Imaging Features of 2019 Novel Coronavirus (2019-nCoV). *Radiology* **2020**, *295*, 202–207. [CrossRef]

30. Ding, X.; Xu, J.; Zhou, J.; Long, Q. Chest CT findings of COVID-19 pneumonia by duration of symptoms. *Eur. J. Radiol.* **2020**, *127*, 109009. [CrossRef]

31. Cao, Y.; Han, X.; Gu, J.; Li, Y.; Liu, J.; Alwalid, O.; Cui, Y.; Zhang, X.; Zheng, C.; Fan, Y.; et al. Prognostic value of baseline clinical and HRCT findings in 101 patients with severe COVID-19 in Wuhan, China. *Sci. Rep.* **2020**, *10*, 17543. [CrossRef]

32. Available online: https://www.bsti.org.uk/media/resources/files/BSTI_COVID-19_Radiology_Guidance_version_2_16.03.20.pdf (accessed on 11 September 2023).

33. Amini, B.; Vadera, S. Ground-Glass Opacification. Reference Article. 2023. Available online: https://radiopaedia.org/articles/ground-glass-opacification-3?lang=us (accessed on 4 September 2022).

34. De Wever, W.; Meersschaert, J.; Coolen, J.; Verbeken, E.; Verschakelen, J.A. The crazy-paving pattern: A radiological-pathological correlation. *Insights Imaging* **2011**, *2*, 117–132. [CrossRef]

35. Hashemi-Madani, N.; Emami, Z.; Janani, L.; Khamseh, M.E. Typical chest CT features can determine the severity of COVID-19: A systematic review and meta-analysis of the observational studies. *Clin. Imaging* **2021**, *74*, 67–75. [CrossRef]

36. Zakariaee, S.S.; Salmanipour, H.; Naderi, N.; Kazemi-Arpanahi, H.; Shanbehzadeh, M. Association of chest CT severity score with mortality of COVID-19 patients: A systematic review and meta-analysis. *Clin. Transl. Imaging* **2022**, *10*, 663–676. [CrossRef] [PubMed]

37. Wang, R.; Jiao, Z.; Yang, L.; Choi, J.W.; Xiong, Z.; Halsey, K.; Tran, T.M.L.; Pan, I.; Collins, S.A.; Feng, X.; et al. Artificial intelligence for prediction of COVID-19 progression using CT imaging and clinical data. *Eur. Radiol.* **2022**, *32*, 205–212. [CrossRef]

38. Lessmann, N.; Sánchez, C.I.; Beenen, L.; Boulogne, L.H.; Brink, M.; Calli, E.; Charbonnier, J.-P.; Dofferhoff, T.; van Everdingen, W.M.; Gerke, P.K.; et al. Automated Assessment of COVID-19 Reporting and Data System and Chest CT Severity Scores in Patients Suspected of Having COVID-19 Using Artificial Intelligence. *Radiology* **2021**, *298*, E18–E28. [CrossRef]

39. Tsakok, M.T.; Watson, R.A.; Saujani, S.J.; Kong, M.; Xie, C.; Peschl, H.; Wing, L.; MacLeod, F.K.; Shine, B.; Talbot, N.P.; et al. Chest CT and Hospital Outcomes in Patients with Omicron Compared with Delta Variant SARS-CoV-2 Infection. *Radiology* **2022**, *306*, 220533. [CrossRef]

40. Verma, A.; Kumar, I.; Singh, P.K.; Ansari, M.S.; Singh, H.A.; Sonkar, S.; Prakash, A.; Ojha, R. Initial comparative analysis of pulmonary involvement on HRCT between vaccinated and non-vaccinated subjects of COVID-19. *Eur. Radiol.* **2022**, *32*, 4275–4283. [CrossRef]
41. Peduzzi, P.; Concato, J.; Kemper, E.; Holford, T.R.; Feinstein, A.R. A simulation study of the number of events per variable in logistic regression analysis. *J. Clin. Epidemiol.* **1996**, *49*, 1373–1379. [CrossRef] [PubMed]